Theoretical physics.
Physics of atoms and molecules

UDC 539.1

EDN QEBNZO
https://www.doi.org/10.33910/2687-153X-2023-4-3-124-130

Atomic data on inelastic collisional process for YH

V. A. Vasileva[1], S. A. Yakovleva✉[1]

[1] Herzen State Pedagogical University of Russia, 48 Moika Emb., Saint Petersburg 191186, Russia

Authors

Vera A. Vasileva, ORCID: 0009-0009-9622-9128, e-mail: veravasilieva2000@gmail.ru

Svetlana A. Yakovleva, ORCID: 0000-0002-8889-7283, e-mail: cvetaja@gmail.com

For citation: Vasileva, V. A., Yakovleva, S. A. (2023) Atomic data on inelastic collisional process for YH. *Physics of Complex Systems*, 4 (3), 124–130. https://www.doi.org/10.33910/2687-153X-2023-4-3-124-130 EDN QEBNZO

Received 9 June 2023; reviewed 5 July 2023; accepted 5 July 2023.

Funding: This study was supported by the Russian Science Foundation (the Russian Federation), Project No. 22-23-01181.

Abstract. The cross sections and rate coefficients for inelastic processes in low-energy collisions of yttrium and hydrogen atoms and ions are calculated. Three ionic states of $Y^+ + H^-$ are considered. Calculations of non-adiabatic nuclear dynamics in all molecular symmetries of each ionic state are performed. Inelastic processes due to non-adiabatic transitions between 65 different states of the YH quasimolecule are considered. In total, 1,796 inelastic processes are treated and their cross sections for collision energy range from 0.001 to 100 eV and rate coefficients for temperatures from 1,000 to 10,000 K are calculated and analyzed. Inelastic processes with large rate coefficients are important for treating Non-LTE effects in astrophysical modeling.

Keywords: atomic data, inelastic processes, non-adiabatic transitions, yttrium, hydrogen

Introduction

Chemical elements that are formed in neutron-capture processes (n-processes) such as Sr, Ba, Y, La, Zr are of great interest to astrophysical studies. The information on the abundances of these elements in stars and star clusters is important in order to understand n-processes as a source of gaseous environment enrichment (Busso et al. 2001), chemical evolution of galactic disks (Chiappini, Gratton 1997; Serminato et al. 2009) and the production of star clusters (Brewer, Carney 2006).

Neutron capture involves two main processes that depend on the density of the neutron flux: a slow process (s-process) and a rapid process (r-process). The main sources of elements produced in neutron capture (primarily, yttrium and barium) are stars with small and intermediate masses in the asymptotic giant branch. They enrich the interstellar medium with these chemical elements that enter stars during their formation (Travaglio et al. 1999).

In astrophysical modeling of various gaseous environments, a model atom for each chemical element is constructed. It includes energy levels and the data on radiative and non-radiative inelastic processes due to collisions with electrons, atoms, and molecules. Collisions of different atoms and ions with hydrogen atoms and negative ions are one of the greatest uncertainties in astrophysical modeling as hydrogen is the most abundant element in the universe. For this reason, a theoretical calculation of molecular data on inelastic hydrogen collisions is important for astrophysics.

Brief theory

Inelastic processes in collisions of yttrium atoms and positive ions and hydrogen atoms and negative ions are studied within the Born-Oppenheimer formalism using asymptotic model approach (Belyaev 2013).

This approach allows to model non-adiabatic regions due to ionic-covalent interaction via constructing the electronic Hamiltonian matrix in the diabatic representation. The diagonal matrix elements are the diabatic potential energies determined by the Coulomb potential in case of the ionic term and by the asymptotic energy of the scattering channel in case of the covalent term; off-diagonal matrix elements that represent ionic-covalent interaction are calculated using a semi-empirical formula from (Olson et al. 1971).

Non-adiabatic nuclear dynamics is treated within the Landau-Zener multichannel model. Transition probabilities in one non-adiabatic region are calculated using an adiabatic potential-based formula (Belyaev, Lebedev 2011), while state-to-state transition probability $p_{if}(J, E)$ for a particular collision energy E and total angular momentum quantum number J is calculated using analytical expressions that take all non-adiabatic regions into account (Yakovleva et al. 2016). Inelastic cross sections $\sigma_{if}(E)$ and rate coefficients K_{if} for exothermic processes ($i > f$) are then calculated using the following equations:

$$\sigma_{if}(E) = \frac{\pi\hbar^2 p_i^{stat}}{2\mu E}\sum_{J=0}^{J_{max}} P_{if}(J,E)(2J+1),$$

$$K_{if} = \sqrt{\frac{8}{\pi\mu(k_B T)^3}}\int_0^\infty \sigma_{if}(E)E\exp\left(-\frac{E}{k_B T}\right)dE,$$

where μ is the reduced nuclear mass, p_i^{stat} is the statistical probability of population of the initial channel i, k_B is the Boltzmann constant. For endothermic processes ($k < j$) cross sections and rate coefficients are calculated using detailed balance equations:

$$\sigma_{kj}(E) = \sigma_{kj}(E+\Delta E_{kj})\frac{p_k^{stat}}{p_j^{stat}}\frac{E+\Delta E_{kj}}{E},$$

$$K_{kj}(T) = K_{jk}(T)\frac{p_k^{stat}}{p_j^{stat}}\exp\left(\frac{\Delta E_{kj}}{k_B T}\right),$$

where ΔE_{kj} is the energy defect between the asymptotic energies E_k and E_j.

YH calculations

The present study of inelastic processes in ytterbium-hydrogen collisions is performed for three sets of molecular states. As the asymptotic model approach (Belyaev 2013) allows taking into account only ionic-covalent interaction, we include only those covalent molecular states that have the same molecular symmetries. Each set contains one of the ionic molecular terms $Y^+ + H^-$ and the covalent molecular states that have the same core electrons configuration. All the molecular states, corresponding scattering channels and asymptotic energies for these tree sets are summarized in Tables 1, 2 and 3:

Table 1: 5 covalent $Y(5s^2\,{}^2L) + H(1s\,{}^2S)$ molecular states and ionic state $Y^+(5s^2\,{}^1S) + H^-(1s^2\,{}^1S)$ with ${}^1\Sigma^+$ molecular symmetry;

Table 2: 35 covalent $Y(4d5s\,{}^{2,4}L) + \mathrm{H}(1s\,{}^2S)$ molecular states and ionic state $Y^+(4d5s\,{}^3D) + H^-(1s^2\,{}^1S)$ with ${}^3\Sigma^+$, ${}^3\Pi$, ${}^3\Delta$ molecular symmetries;

Table 3: 22 covalent $Y(4d5s\,{}^{1,3}L) + H(1s^2S)$ molecular states and ionic state $Y^+(4d5s\,{}^1D) + \mathrm{H}^-(1s^2\,{}^1S)$ with ${}^1\Sigma^+$, ${}^1\Pi$, ${}^1\Delta$, molecular symmetries.

Table 1. The $Y({}^2L) + H(1s\,{}^2S)$ and $Y^+(5s^2\,{}^1S) + H^-(1s^2\,{}^1S)$ molecular channels, the corresponding asymptotic atomic states, and the asymptotic energies with respect to the ground state

j	Asymptotic atomic states	Molecular symmetries	Asymptotic energies (eV)
1	$Y(4d5s^2\,{}^2D) + H(1s\,{}^2S)$	${}^1\Sigma^+$	0.03885
2	$Y(5s^2\,5p\,{}^2P) + H(1s\,{}^2S)$	${}^1\Sigma^+$	1.37165
3	$Y(5s^2\,6s\,{}^2S) + H(1s\,{}^2S)$	${}^1\Sigma^+$	3.92677

Table 1. Completion

4	$Y(5s^2\ (^2D)5d\ ^2D) + H(1s\ ^2S)$	$^1\Sigma^+$	4.24606
5	$Y(5s^2\ (^1S\ )6p\ ^2P) + H(1s\ ^2S)$	$^1\Sigma^+$	4.61472
ionic	$Y+\ (5s^2\ ^1S) + H-\ (1s^2\ ^1S)$	$^1\Sigma^+$	5.46326

Table 2. The $Y(^{2,4}L) + H(1s\ ^2S)$ and $Y^+(4d5s\ ^3D) + H^-(1s^2\ ^1S)$ molecular channels, the corresponding asymptotic atomic states, and the asymptotic energies with respect to the ground state

j	Asymptotic atomic states	Molecular symmetries			Asymptotic energies (eV)
1	$Y(4d5s^2\ ^2D) + H(1s\ ^2S)$	$^3\Sigma^+$	$^3\Pi$	$^3\Delta$	0.03885
2	$Y(4d^2(^3F)5s\ ^4F) + H(1s\ ^2S)$	–	$^3\Pi$	$^3\Delta$	1.39762
3	$Y(4d^2\ (^3P)5s\ ^4P) + H(1s\ ^2S)$	–	$^3\Pi$	–	1.90689
4	$Y(4d^2\ (^3F)5s\ ^2F) + H(1s\ ^2S)$	–	$^3\Pi$	$^3\Delta$	1.93805
5	$Y(4d5s(^3D)5p\ ^4F) + H(1s\ ^2S)$	$^3\Sigma^+$	$^3\Pi$	$^3\Delta$	1.94401
6	$Y(4d^2\ (^1D)5s\ ^2D) + H(1s\ ^2S)$	$^3\Sigma^+$	$^3\Pi$	$^3\Delta$	1.99508
7	$Y(4d5s(^3D)5p\ ^2D) + H(1s\ ^2S)$	–	$^3\Pi$	$^3\Delta$	1.99599
8	$Y(4d5s(^3D)5p\ ^4D) + H(1s\ ^2S)$	–	$^3\Pi$	$^3\Delta$	2.08841
9	$Y(4d^2(^1G)5s\ ^2G) + H(1s\ ^2S)$	$^3\Sigma^+$	$^3\Pi$	$^3\Delta$	2.29434
10	$Y(4d5s(^3D)5p\ ^4P) + H(1s\ ^2S)$	$^3\Sigma^+$	$^3\Pi$	–	2.36513
11	$Y(4d^2\ (^3P)5s\ ^2P) + H(1s\ ^2S)$	–	$^3\Pi$	–	2.39859
12	$Y(4d5s(^3D)5p\ ^2F) + H(1s\ ^2S)$	$^3\Sigma^+$	$^3\Pi$	$^3\Delta$	2.69638
13	$Y(4d^2(^1S)5s\ ^2S) + H(1s\ ^2S)$	$^3\Sigma^+$	–	–	2.90930
14	$Y(4d5s(^3D)5p\ ^2P) + H(1s\ ^2S)$	$^3\Sigma^+$	$^3\Pi$	–	3.04487
15	$Y(4d5s(^1D)5p\ ^2F) + H(1s\ ^2S)$	$^3\Sigma^+$	$^3\Pi$	$^3\Delta$	3.06669
16	$Y(4d5s(^1D)5p\ ^2D) + H(1s\ ^2S)$	–	$^3\Pi$	$^3\Delta$	3.06818
17	$Y(4d5s(^1D)5p\ ^2P) + H(1s\ ^2S)$	$^3\Sigma^+$	$^3\Pi$	–	3.47492
18	$Y(4d5s(^3D)6s\ ^4D) + H(1s\ ^2S)$	$^3\Sigma^+$	$^3\Pi$	$^3\Delta$	4.15074
19	$Y(4d5s(^3D)6s\ ^2D) + H(1s\ ^2S)$	$^3\Sigma^+$	$^3\Pi$	$^3\Delta$	4.51635
20	$Y(4d5s(^1D)6s\ ^2D) + H(1s\ ^2S)$	$^3\Sigma^+$	$^3\Pi$	$^3\Delta$	4.58576
21	$Y(4d5s(^3D)5d\ ^4D) + H(1s\ ^2S)$	$^3\Sigma^+$	$^3\Pi$	$^3\Delta$	4.79801
22	$Y(4d5s(^3D)6p\ ^4D) + H(1s\ ^2S)$	–	$^3\Pi$	$^3\Delta$	4.81911
23	$Y(4d5s(^3D)6p\ ^4F) + H(1s\ ^2S)$	$^3\Sigma^+$	$^3\Pi$	$^3\Delta$	4.82798
24	$Y(4d5s(^3D)5d\ ^4G) + H(1s\ ^2S)$	$^3\Sigma^+$	$^3\Pi$	$^3\Delta$	4.82840
25	$Y(4d5s(^3D)6p\ ^2F) + H(1s\ ^2S)$	$^3\Sigma^+$	$^3\Pi$	$^3\Delta$	4.83337
26	$Y(4d5s(^3D)5d\ ^4S) + H(1s\ ^2S)$	$^3\Sigma^+$	–	–	4.83556
27	$Y(4d5s(^3D)5d\ ^2P) + H(1s\ ^2S)$	–	$^3\Pi$	–	4.85594
28	$Y(4d5s(^3D)6p\ ^2D) + H(1s\ ^2S)$	–	$^3\Pi$	$^3\Delta$	4.86874
29	$Y(4d5s(^3D)6p\ ^4P) + H(1s\ ^2S)$	$^3\Sigma^+$	$^3\Pi$	–	4.90231
30	$Y(4d5s(^3D)5d\ ^4F) + H(1s\ ^2S)$	–	$^3\Pi$	$^3\Delta$	4.92456
31	$Y(4d5s(^3D)5d\ ^2F) + H(1s\ ^2S)$	–	$^3\Pi$	$^3\Delta$	4.92681
32	$Y(4d5s(^3D)5d\ ^4P) + H(1s\ ^2S)$	–	$^3\Pi$	–	5.01564

https://www.doi.org/10.33910/2687-153X-2023-4-3-124-130

Table 2. Completion

33	$Y(4d5s(^3D)5d\ ^2D) + H(1s\ ^2S)$	–	$^3\Pi$	$^3\Delta$	5.14169
34	$Y(4d5s(^1D)5d\ ^2D) + H(1s\ ^2S)$	$^3\Sigma^+$	$^3\Pi$	$^3\Delta$	5.16591
35	$Y(4d5s(^1D)5d\ ^2P) + H(1s\ ^2S)$	–	$^3\Pi$	–	5.29103
ionic	$Y^+(4d5s\ ^3D) + H^-(1s^2\ ^1S)$	$^3\Sigma^+$	$^3\Pi$	$^3\Delta$	5.61116

Table 3. The $Y(^{1,3}L) + H(1s\ ^2S)$ and $Y^+(4d5s\ ^1D) + H^-(1s^2\ ^1S)$ molecular channels, the corresponding asymptotic atomic states, and the asymptotic energies with respect to the ground state

j	Asymptotic atomic states	Molecular symmetries			Asymptotic energies (eV)
1	$Y(4d5s^2\ ^2D) + H(1s\ ^2S)$	$^1\Sigma^+$	$^1\Pi$	$^1\Delta$	0.03885
2	$Y(4d^2(^3F)5s\ ^2F) + H(1s\ ^2S)$	–	$^1\Pi$	$^1\Delta$	1.93805
3	$Y(4d^2(^1D)5s\ ^2D) + H(1s\ ^2S)$	$^1\Sigma^+$	$^1\Pi$	$^1\Delta$	1.99508
4	$Y(4d5s(^3D)5p\ ^2D) + H(1s\ ^2S)$	–	$^1\Pi$	$^1\Delta$	1.99599
5	$Y(4d^2(^1G)5s\ ^2G) + H(1s\ ^2S)$	$^1\Sigma^+$	$^1\Pi$	$^1\Delta$	2.29434
6	$Y(4d^2(^3P)5s\ ^2P) + H(1s\ ^2S)$	–	$^1\Pi$	–	2.39859
7	$Y(4d5s(^3D)5p\ ^2F) + H(1s\ ^2S)$	–	$^1\Pi$	$^1\Delta$	2.69638
8	$Y(4d2(^1S)5s\ ^2S) + H(1s\ ^2S)$	$^1\Sigma^+$	–	–	2.90930
9	$Y(4d5s(^3D)5p\ ^2P) + H(1s\ ^2S)$	$^1\Sigma^+$	$^1\Pi$	–	3.04487
10	$Y(4d5s(^1D)5p\ ^2F) + H(1s\ ^2S)$	$^1\Sigma^+$	$^1\Pi$	$^1\Delta$	3.06669
11	$Y(4d5s(^1D)5p\ ^2D) + H(1s\ ^2S)$	–	$^1\Pi$	$^1\Delta$	3.06818
12	$Y(4d5s(^1D)5p\ ^2P) + H(1s\ ^2S)$	$^1\Sigma^+$	$^1\Pi$	–	3.47492
13	$Y(4d5s(^3D)6s\ ^2D) + H(1s\ ^2S)$	$^1\Sigma^+$	$^1\Pi$	$^1\Delta$	4.51635
14	$Y(4d5s(^1D)6s\ ^2D) + H(1s\ ^2S)$	$^1\Sigma^+$	$^1\Pi$	$^1\Delta$	4.58576
15	$Y(4d5s(^3D)6p\ ^2F) + H(1s\ ^2S)$	$^1\Sigma^+$	$^1\Pi$	$^1\Delta$	4.83337
16	$Y(4d5s(^3D)5p\ ^2P) + H(1s\ ^2S)$	–	$^1\Pi$	–	4.85594
17	$Y(4d5s(^3D)6p\ ^2D) + H(1s\ ^2S)$	–	$^1\Pi$	$^1\Delta$	4.86874
18	$Y(4d5s(^3D)5d\ ^2F) + H(1s\ ^2S)$	–	$^1\Pi$	$^1\Delta$	4.92681
19	$Y(4d5s(^3D)5d\ ^2D) + H(1s\ ^2S)$	$^1\Sigma^+$	$^1\Pi$	$^1\Delta$	5.14169
20	$Y(4d5s(^1D)5d\ ^2D) + H(1s\ ^2S)$	$^1\Sigma^+$	$^1\Pi$	$^1\Delta$	5.16591
21	$Y(4d5s(^1D)5d\ ^2P) + H(1s\ ^2S)$	–	$^1\Pi$	–	5.29103
22	$Y(4d5s(^1D)5d\ ^2F) + H(1s\ ^2S)$	–	$^1\Pi$	$^1\Delta$	5.46192
ionic	$Y^+(4d5s\ ^1D) + H^-(1s^2\ ^1S)$	$^1\Sigma^+$	$^1\Pi$	$^1\Delta$	5.87193

The data for the atomic levels of yttrium atom and ion and their energy values are taken from NIST (Kramida et al. 2022). Asymptotic energies are averaged over the total angular momentum quantum number *J*. It is worth noting that only one-electron transitions are included in the present investigation as two-electron transitions generally have negligible probabilities, cross sections and rate coefficients because of the narrow non-adiabatic regions (Belyaev et al. 2016; 2019; Vlasov et al. 2018).

For all the transitions between the states in the three sets of molecular states, calculations of partial cross sections and rate coefficients are performed within each molecular symmetry separately and then summed over initial and final states of the process. Cross sections are calculated for the collision energy range from 0.01 eV to 100 eV and rate coefficients — for the temperature range from 1,000 K to 10,000 K.

Results and analysis

Graphical representation of rate coefficients for the temperature T = 6,000K for all the treated processes is shown in Figs 1, 2 and 3 for the three sets of molecular states from Tables 1, 2 and 3, respectively. The rate coefficient order of magnitude is shown with color from blue to red (see the respective legend). The initial and final states labels in graphical representations correspond to those in Tables 1, 2 and 3. White color denotes either the elastic processes that are not studied in the present work (diagonal squares) or transitions between molecular states that do not have the same symmetries.

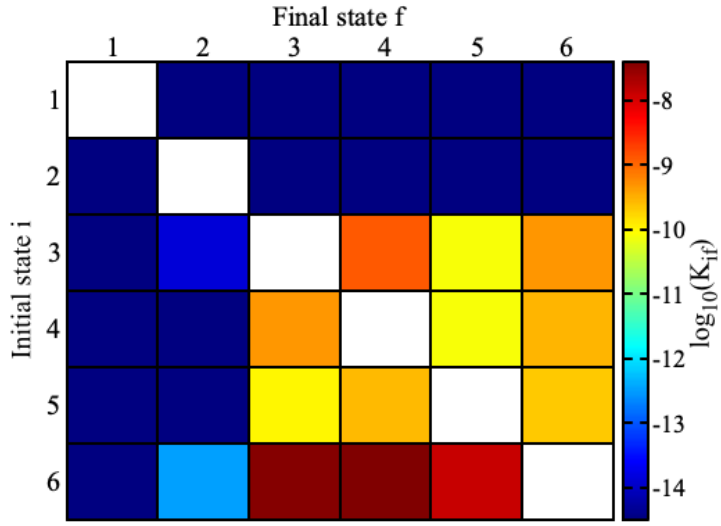

Fig. 1. Graphical representation of the inelastic processes rate coefficients in $Y(^2L) + H(1s\ ^2S)$ and $Y^+(5s^2\ ^1S) + H^-(1s^2\ ^1S)$ collisions. The labels for the initial and final states are given in Table 1.

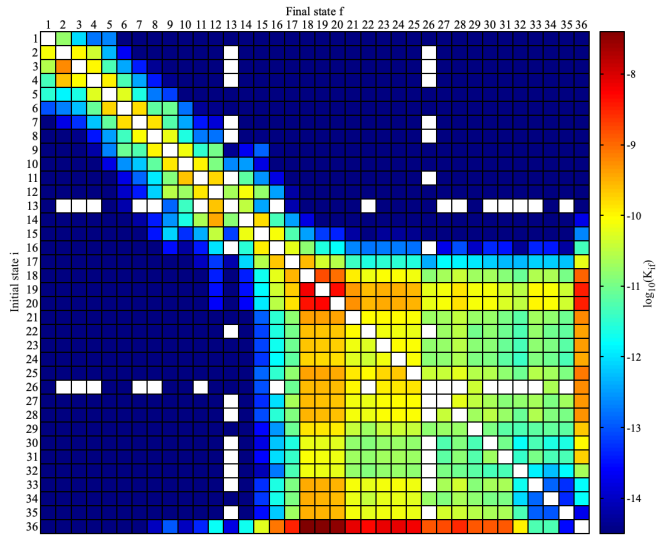

Fig. 2. Graphical representation of the inelastic processes rate coefficients in $Y(^{2,4}L) + H(1s\ ^2S)$ and $Y^+(4d5s\ ^3D) + H^-(1s^2\ ^1S)$ collisions. The labels for the initial and final states are given in Table 2.

 https://www.doi.org/10.33910/2687-153X-2023-4-3-124-130

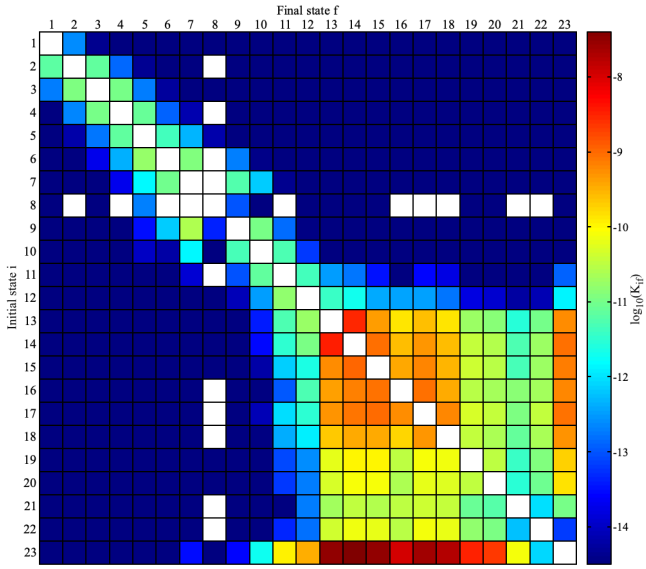

Fig. 3. Graphical representation of the inelastic processes rate coefficients in $Y(^{1,3}L) + H(1s\,^2S)$ and $Y^+(4d5s\,1D) + H^-(1s^2\,^1S)$ collisions. The labels for the initial and final states are given in Table 3.

For the first group of molecular states (see Table 1) the largest rate coefficients at T = 6,000 K correspond the neutralization processes $Y^+(5s^2\,^1S) + H^- \rightarrow Y(5s^2\,nl\;\,^2L) + H$ (j = 6 to j = 3, 4, 5) with values:

$K_{6\rightarrow3} = 3.59 \times 10^{-8}$ cm^3 s^{-1},
$K_{6\rightarrow4} = 5.86 \times 10^{-8}$ cm^3 s^{-1},
$K_{6\rightarrow5} = 1.24 \times 10^{-8}$ cm^3 s^{-1}.

In the second molecular states group (Table 2) the largest rate coefficients at T = 6,000 K correspond the neutralization processes $Y^+(4d5s\,^3D) + H^- \rightarrow Y(4d5s\,nl\,^{2,4}L) + H$ (j = 36 to j = 18, 19, 20) with values:

$K_{36\rightarrow18} = 4.72 \times 10^{-8}$ cm^3 s^{-1},
$K_{36\rightarrow19} = 3.67 \times 10^{-8}$ cm^3 s^{-1},
$K_{36\rightarrow20} = 3.13 \times 10^{-8}$ cm^3 s^{-1}.

In case of the third group (Table 3) the largest rate coefficients at T = 6,000 K correspond the neutralization processes $Y^+(4d5s\,^1D) + H^- \rightarrow Y(4d5s\,nl\,^{1,3}L) + H$ (j = 23 to j = 13 – 18) with values:

$K_{23\rightarrow13} = 3.01 \times 10^{-8}$ cm^3 s^{-1},
$K_{23\rightarrow14} = 4.12 \times 10^{-8}$ cm^3 s^{-1},
$K_{23\rightarrow15} = 2.93 \times 10^{-8}$ cm^3 s^{-1},
$K_{23\rightarrow16} = 1.05 \times 10^{-8}$ cm^3 s^{-1},
$K_{23\rightarrow17} = 2.33 \times 10^{-8}$ cm^3 s^{-1},
$K_{23\rightarrow18} = 1.75 \times 10^{-8}$ cm^3 s^{-1},

Conclusions

The reported study of inelastic yttrium and hydrogen collisions is performed for the three sets of ionic molecular states of $Y^+ + H^-$. For each set, the study of non-adiabatic nuclear dynamics is carried out within all the molecular symmetries of a particular ionic state. Inelastic processes due to nonadiabatic transitions between 65 different states of the YH quasimolecule are considered. In total, 1,796 inelastic processes are studied, cross sections are calculated for the collision energy range from 0.001 eV to 100 eV and the rate coefficients are calculated for temperatures from 1,000 K to 10,000 K. Inelastic processes with large values of the rate coefficients may find application in non-LTE astrophysical modeling.

Conflict of Interest

The authors declare that there is no conflict of interest, either existing or potential.

Author Contributions

All the authors discussed the final work and took an equal part in writing the article.

Acknowledgements

Authors gratefully acknowledge discussions with Prof. Andrey K. Belyaev.

References

Belyaev, A. K. (2013) Model approach for low-energy inelastic atomic collisions and application to Al + H and Al+ + H–. *Physical Review A*, 88 (5), article 052704. https://doi.org/10.1103/PhysRevA.88.052704 (In English)

Belyaev, A. K., Lebedev, O. V. (2011) Nonadiabatic nuclear dynamics of atomic collisions based on branching classical trajectories. *Physical Review A*, 84 (1), article 014701. https://doi.org/10.1103/PhysRevA.84.014701 (In English)

Belyaev, A. K., Vlasov, D. V., Mitrushchenkov, A., Feautrier, N. (2019) Quantum study of inelastic processes in low-energy calcium–hydrogen collisions. *Monthly Notices of the Royal Astronomical Society*, 490 (3), 3384–3391. https://doi.org/10.1093/mnras/stz2763 (In English)

Belyaev, A. K., Yakovleva, S. A., Guitou, M. et al. (2016) Model estimates of inelastic calcium-hydrogen collision data for non-LTE stellar atmospheres modeling. *Astronomy & Astrophysics*, 587, article A114. https://doi.org/10.1051/0004-6361/201527651 (In English)

Brewer, M. M., Carney, B. W. (2006) A comparison of the chemical evolutionary histories of the galactic thin disk and thick disk stellar populations. *The Astronomical Journal*, 131 (1), article 431. https://doi.org/10.1086/498110 (In English)

Busso, M., Gallino, R., Lambert, D. L. et al. (2001) Nucleosynthesis and mixing on the asymptotic giant branch. III. Predicted and observed s-process abundances. *The Astrophysical Journal*, 557 (2), article 802. https://doi.org/10.1086/322258 (In English)

Chiappini, C., Gratton, A. R. (1997) The chemical evolution of the galaxy: The two-infall model. *The Astrophysical Journal*, 477 (2), article 765. https://doi.org/10.1086/303726 (In English)

Kramida, A., Ralchenko, Yu., Reader, J. et al. (2022). NIST Atomic Spectra Database (ver. 5.10). *National Institute of Standards and Technology*. [Online]. Available: https://doi.org/10.18434/T4W30F (accessed 23.04.2023). (In English)

Olson, R. E., Smith, F. T., Bauer, E. (1971) Estimation of the coupling matrix elements for one-electron transfer systems. *Applied Optics*, 10 (8), 1848–1855. https://doi.org/10.1364/AO.10.001848 (In English)

Serminato, A., Gallino, R., Travaglio, C. et al. (2009) Galactic chemical evolution of the s-process from AGB stars. *Publications of the Astronomical Society of Australia*, 26 (3), 153–160. https://doi.org/10.1071/AS08053 (In English)

Travaglio, C., Galli, D., Gallino, R. et al. (1999) Galactic chemical evolution of heavy elements: From barium to europium. *The Astrophysical Journal*, 521 (2), article 691. https://doi.org/10.1086/307571 (In English)

Vlasov, D. V., Rodionov, D. S., Belyaev, A. K. (2018) The hybrid diabatization method and its application to the CaH quasi-molecule. *Optics and Spectroscopy*, 124 (5), 611–617. https://doi.org/10.1134/S0030400X18050223 (In English)

Yakovleva, S. A., Voronov, Ya. V., Belyaev, A. K. (2016) Atomic data on inelastic processes in low-energy beryllium-hydrogen collisions. *Astronomy and Astrophysics*, 593, article A27. https://doi.org/10.1051/0004-6361/201628659 (In English)